

# User-Oriented Human-Robot Interaction for an Intelligent Walking Assistant Robotic Device

Costas S. Tzafestas, Xanthi S. Papageorgiou, George P. Moustris,  
Georgia Chalvatzaki, and Athanasios Dometios

School of Electrical and Computer Engineering, National Technical University of Athens, Greece

ktzaf@cs.ntua.gr, {xpapag, gmoustri}@mail.ntua.gr

**Abstract**—During the past decade, robotic technology has evolved considerably towards the development of cognitive robotic systems that enable close interaction with humans. Application fields of such novel robotic technologies are now wide spreading covering a variety of human assistance functionalities, aiming in particular at supporting the needs of human beings experiencing various forms of mobility or cognitive impairments. Mobility impairments are prevalent in the elderly population and constitute one of the main causes related to difficulties in performing Activities of Daily Living (ADLs) and consequent reduction of quality of life. This paper reports current research work related to the control of an intelligent robotic rollator aiming to provide user-adaptive and context-aware walking assistance. To achieve such targets, a large spectrum of multimodal sensory processing and interactive control modules need to be developed and seamlessly integrated, that can, on one side track and analyse human motions and actions, in order to detect pathological situations and estimate user needs, while predicting at the same time the user (short-term or long-range) intentions in order to adapt robot control actions and supportive behaviours accordingly. User-oriented human-robot interaction and control refers to the functionalities that couple the motions, the actions and, in more general terms, the behaviours of the assistive robotic device to the user in a *non-physical interaction* context.

In this context, this paper presents current advances in two directions, focusing towards the development of: 1) a user monitoring system that can enable tracking, analysis and classification of human gait patterns, based on non-intrusive laser rangefinder data, and 2) a control system that can support a ‘user-following’ behaviour; that is, enable the robotic rollator to follow and comply to the walking characteristics of the user without any physical interaction (i.e. without any force being applied on the handles of the Rollator) and remain in close vicinity to the user in case of need. This paper summarizes the theoretical framework and presents current experimental results obtained using real data both from patients (elderly subjects with mild to moderate walking impairments) and normal subjects. Results are promising demonstrating that such a framework can be used efficiently and effectively to provide user-adapted mobility assistance that can enhance the functionality of such robotic devices.

## I. INTRODUCTION

Elder care constitutes a major issue for modern societies, as the elderly population constantly increases [1]. Mobility problems are common in seniors. As people age they have to cope with instability and lower walking speed [2]. It is well known that mobility impairments constitute a key factor impeding many activities of daily living important to independent living, having a strong impact in productive

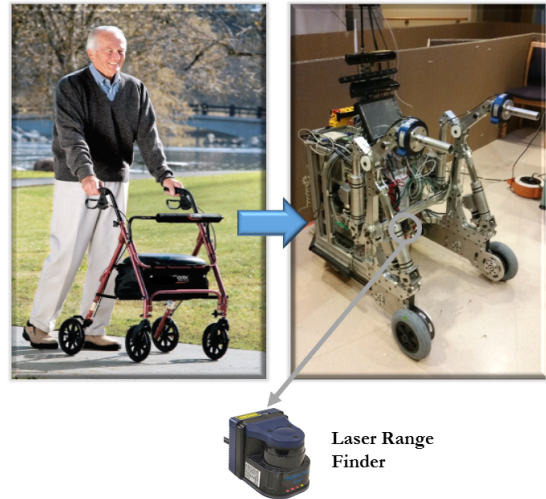


Fig. 1: Left: Typical passive assistive device for elderly. Right: The robotic platform based on the rollator prototype equipped with a Hokuyo Laser Sensor aiming to record user’s gait data.

life, independence, physical exercise, and self-esteem [3], [4]. Most people with mobility issues, patients or elders, have to use walkers in their everyday activities and they need the constant supervision of a carer. The social and economic significance of solving these issue should not be underestimated. Robotics seems to fit naturally to the role of assistance since it can incorporate features such as posture support and stability enhancement, walking assistance, navigation and cognitive assistance in indoor and outdoor environments, health monitoring etc.

This paper reports research work conducted in the frames of an EU funded research project MOBOT, aiming to develop an intelligent robotic rollator aiming to provide user-adaptive and context-aware walking assistance (see Fig. 1). The main motivation behind this work derives from our vision of developing and advancing robotic technologies enabling the development and deployment of cognitive assistive devices that can monitor and understand specific forms of human walking activities in their workspace, in order to deduce the particular needs of a user regarding mobility and ambulation. The ultimate goal is to provide context-aware support [5],

and intuitive, user-adapted assistance to users experiencing mild to moderate mobility and/or cognitive impairments in domestic environments. To achieve such targets, a large spectrum of multimodal sensory processing and interactive control modules need to be developed and seamlessly integrated, that can, on one side track and analyse human motions and actions, in order to detect pathological situations and estimate user needs, while predicting at the same time the user (short-term or long-range) intentions in order to adapt robot control actions and supportive behaviours accordingly. User-oriented human-robot interaction and control refers to the functionalities that couple the motions, the actions and, in more general terms, the behaviours of the assistive robotic device to the user in a *non-physical interaction* context.

In this paper, we summarise current research work, focusing on recent advances and challenges in two directions:

1) First of all, we address the challenge of developing a reliable pathological walking assessment system, that can operate on-line and in real-time enabling the robotic assistive device to continuously monitor and analyse the gait characteristics of the user in order to recognise walking patterns that can be classified as pathological requiring specific attention and handling by the system. The proposed system uses an onboard laser rangefinder sensor to detect and track user legs (a non-intrusive solution that does not interfere with human motion). A hidden Markov model (HMM) approach is used to perform statistical modeling of human gait. This paper presents the results of this gait modeling framework in terms of segmenting the gait cycle and recognising different gait phases, which can be subsequently used to extract gait parameters. This paper presents preliminary gait characterisation results for five patients, from a full-scale experimental study conducted at the premises of the Bethanien Hospital - Geriatric Centre of the University of Heidelberg, at the frames of the EU-funded FP7 research project MOBOT.

2) Secondly, we focus on the development of a control system that can support a ‘user-following’ behaviour; that is, enable the robotic rollator to follow and comply to the walking characteristics of the user without any physical interaction (i.e. without any force being applied on the handles of the Rollator) and remain in close vicinity to the user in case of need. This paper summarizes the theoretical framework and presents current experimental results obtained using real data both from patients (elderly subjects with mild to moderate walking impairments) and normal subjects. Results are promising demonstrating that such a framework can be used efficiently and effectively to provide user-adapted mobility assistance that can enhance the functionality of such robotic devices.

This paper summarizes the theoretical framework and presents current experimental results obtained using real data both from patients (elderly subjects with mild to moderate walking impairments) and normal subjects. With respect to gait analysis and assessment, as opposed to most of the literature available on the topic, the approach presented in this paper is completely non-intrusive based on the use of a typical non-wearable device. Instead of using complex



Fig. 2: Internal gait phases of human normal gait cycle.

models and motion tracking approaches that require expensive or bulky sensors and recording devices that interfere with human motion, the measured data used in this work is provided by a standard laser rangefinder sensor mounted on the prototype robotic rollator platform. In this paper, we perform an initial assessment of an HMM-based methodology used for the statistical modeling and classification of human gait patterns and for the extraction of clinically-relevant gait parameters.

This paper also summarizes the methodological framework enabling a user front-following behaviour for the robotic rollator. The current methodology implements a kinematic human-robot interaction control approach, essentially regulating a virtual pushing behavior. Experiments with real users have shown that even though this control behavior is successful, it inserts a cognitive load on the users who try to steer the robot on the optimal path they would have taken under normal conditions. As a result, the users deviate from their normal gait pattern in their effort to control the robot. Current research focuses on the development of a shared control user-assistance behaviour. Our approach considers user intent recognition by introducing the concept of dynamic undecidability, and employs a dynamic window method for local kinodynamic planning.

The experimental results presented in this paper are promising, demonstrating that such a framework can be used efficiently and effectively to provide user-adapted mobility assistance that can enhance the functionality of such robotic devices. The ultimate objective of this work is to design a reliable pathological walking assessment system (that embodies several walking morphologies, allowing inclusion of new patients with different mobility pathologies) and incorporate this tracking and monitoring system in a context-aware robot control framework enabling a cognitive mobility assistance robotic device to provide user-adaptive walking support actions and intuitive assistive behaviours.

The paper is organised as follows. Section II describes the proposed HMM-based gait analysis and characterisation framework, while Section III summarises the user front-

following methodology adopted in current experiments. Section IV describes the experimental results achieved regarding both the gait analysis and the user-following control modules, while Section V presents conclusions and summarises future research work directions.

## II. HMM-BASED GAIT ANALYSIS

For gait recognition purposes we have used Hidden Markov models (HMMs). An HMM has well suited statistical properties, and it is able to capture the temporal state-transition nature of gait. In our previous work, we have proposed and analyzed extensively the properties of an HMM system and its applications for modelling normal human gait [6], as well as for pathological gait recognition [7]. The proposed model uses a seven-state representation that follows the typical definition of stance and swing phase events for normal human gait, which are depicted in Fig. 2.

This paper focuses on performing an initial assessment of this framework in terms of extracting clinically-relevant gait parameters that could be used for the characterisation and classification of specific pathological walking patterns. Gait Analysis literature uses specific gait parameters for the quantification of each gait cycle, commonly used for medical diagnosis, [8], [9]. In this work, we are using two temporal parameters: a. **stride time**: the duration of each gait cycle, b. **swing time**: the swing phase duration in a gait cycle, and, one spatial parameter: c. **stride length**, i.e. the distance travelled by both feet in a gait cycle. The rest of this section summarises the methodological background of the proposed HMM framework for gait analysis and characterisation.

### A. User's legs Detection and Tracking

The raw laser data are processed by the detection and tracking system. Each time frame this system estimates the position and velocity of the user's legs with respect to the robotic platform motion. Thus, we mainly utilize K-means clustering and Kalman Filtering (KF) for the estimation of the central positions and velocities of the left and right leg of the user along the axes, [7].

Every time instant, a background extraction of the raw laser data is performed for deleting outliers and then a simple method for grouping laser points based on experimental thresholds is applied. When we end up with two groups, we perform the K-means clustering algorithm, in order to assign each laser group the left/right leg label. Circle Fitting is then used for computing the legs' centers. Those centers are the observation vector that enters a constant acceleration KF. The KF tracks the central positions of the limbs by stochastically estimating their position and velocity. We seed the next detection frame with the prior information of the predicted legs' position and variability. When one leg is occluded by the other while turning, we have a false detection case and we do not use the corresponding laser information for the observation vector. To overcome such situations, we only apply the prediction step of the KF, as we do not observe abrupt changes of the legs' velocity frame-by-frame. The

estimated positions and velocities are the features used in the HMM recognition system.

### B. HMM Gait Cycle Recognition

The hidden states of the HMM are defined by the seven gait phases, Fig. 2. As observables, we utilize several quantities that represent the motion of the subjects' legs, (relative position w.r.t. the laser, velocities, etc.), which are estimated using sequential signals from a laser sensor. The state and observations at time  $t$  are denoted as  $s_t$  and  $O_t$ , respectively. The seven states at time  $t = 1, 2, \dots, T$ , where  $T$  is the total time, are expressed by the value of the (hidden) variable  $s_t = i$ , for  $i = 1, \dots, 7$ , where  $1 \equiv IC/TW$ ,  $2 \equiv LR$ ,  $3 \equiv MS$ ,  $4 \equiv TS$ ,  $5 \equiv PW$ ,  $6 \equiv IW$ , and  $7 \equiv MW$ . The observations at time  $t$ , are represented by the vector  $O_t = [o_t^1 \dots o_t^k]^T$ , for  $k = 1, \dots, 9$ , where  $o_t^1 \equiv x^R$ ,  $o_t^2 \equiv y^R$ ,  $o_t^3 \equiv x^L$ ,  $o_t^4 \equiv y^L$ ,  $o_t^5 \equiv v_x^R$ ,  $o_t^6 \equiv v_y^R$ ,  $o_t^7 \equiv v_x^L$ ,  $o_t^8 \equiv v_y^L$ , and  $o_t^9 \equiv Dlegs$ . The quantities  $(x^R, y^R, x^L, y^L)$  are the positions and  $(v_x^R, v_y^R, v_x^L, v_y^L)$  are the velocities of the right and left leg along the axes, and  $Dlegs$  is the distance between the legs. The observation data are modeled using a mixture of Gaussian distributions.

### C. Gait Parameters Computation

For the computation of the gait parameters from the laser data, we use the time segmentation given by the HMM recognition system. Each recognised gait cycle provides the stride time, while the swing time is the duration of the phases from **IW** to **MW**. The stride length is computed by summing the distances travelled by each leg in the direction towards the robotic platform.

## III. USER FRONT-FOLLOWING

The problem of following from the front can be divided into two general cases; following the human in free space i.e. in an obstacle-free space and, following the human in a structured environment e.g. in an office building, corridor etc. The two problems have different complexity with the former being substantially simpler than the latter. Specifically, in *free space following*, the problem can be cast as a control problem where the goal is to minimize some error measures e.g. minimize the distance and orientation errors between the human and the robot. This approach is singularly treated in the current literature. In the *structured environment* case, the task involves avoiding obstacles, either static or moving, as well as deciding where the human actually wants to go; a possibly undecidable problem. See for example Fig.1.

It is clear that the robot has no way of knowing where the human wants to turn by examining solely the human motion. This problem requires the addition of further information into the control loop by letting the human show the robot to turn left/right using some kind of feedback e.g. audio, posture, gestures etc. Thus, the human must also steer the robot and not just act as an observable for the robot. The control strategy for this problem is radically different from the *free space following* problem, and has received no attention in the literature.

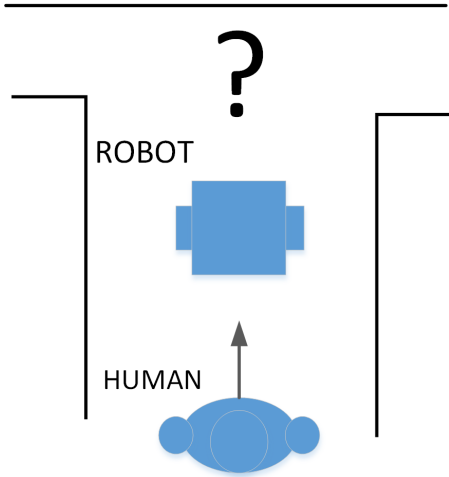


Fig. 3: Undecidability of the front-following problem in structured environments

The front-following problem has received scarce attention from the research community. Our survey has produced only three papers dealing with subject. All three deal with the free-space following problem. In [10] the authors use a Laser Range Finder (LRF) to scan the human torso, which serves as a more robust scanning target than the legs. Using a particle filter employing a constant velocity model, they track the pose of the human during motion. The control algorithm uses a *virtual target* based on the human and robot poses. The aim is for the robot to track the target, which lays in the approximate direction of the human velocity vector. [11] use an RGBD sensor (Microsoft Kinect) to track the human position relative to the robot. Following, they use the nonholonomic human model [12], [13] to calculate the humans orientation, combined with an Unscented Kalman Filter to provide a smooth estimate of the human orientation, linear velocity and angular velocity. The controller is an ad-hoc solution aiming to align the human-robot poses while putting the robot in front. [14] combine readings from a wearable IMU sensor on the human, along with LRF data of the legs in order to provide an estimate of the human pose and linear/angular velocities. They use an inverse kinematics controller to exponentially stabilize a position and orientation error between the human and the robot. In this setup, they perform experiments in straight line tracking, as well as in tracking the human along an 8-shaped path.

#### A. Human pose estimation

The first step towards human following is the detection/estimation of the human pose. A basic assumption is that the human is detected by a LRF located on the robot, which scans the user legs. Furthermore, the kinematic controller only needs the position of the human, not the orientation and velocity. This simplifies the control and is more robust to estimation errors. To filter out environment artefacts and obstacles, we borrow the idea of a Human Interaction Zone

(HIZ) from [14], which consists of a parallelogram of width 2m and length 2m, centered at the LRF. Based on the laser scans inside the HIZ, a *centroid* is calculated by taking the average in each  $x,y$  coordinates. Thus, if  $k$  scans lay inside the HIZ, the centroid coordinates are,

$$\begin{bmatrix} x_H \\ y_H \end{bmatrix} = \begin{bmatrix} 1/k \sum_k x_L^i \\ 1/k \sum_k y_L^i \end{bmatrix} \quad (1)$$

To enable more valid detection results, in order to exclude false positives from walls, furniture etc. we have inserted an adaptive algorithm based on the previous valid centroid position. Specifically, in the beginning, the robot considers only scans inside an *initial window*, similar to the HIZ but with a width of 0.8m. This implies that the human who is intended to be followed, approaches the robot in a narrow region. Following, the algorithm estimates the centroid coordinates  $[x_H^i, y_H^i]$  at loop  $i$ . In the next loop  $i+1$ , the algorithm scans inside a small *leg window*, of width 0.3m and height 0.2m. Thus the detection area is the rectangle  $[x_H^i \pm 0.3, y_H^i \pm 0.2]$ . In this way, the algorithm tracks the human as he/she moves inside the HIZ, and discards other unrelated objects.

#### B. Kinematic controller

The proposed solution for the front-following problem, is a *virtual pushing* approach through a kinematic controller. We define an equilibrium distance  $x_0$  where the system is at rest. If the human passes the equilibrium point and approaches the robot, then the robot starts to move depending on the human-robot distance.

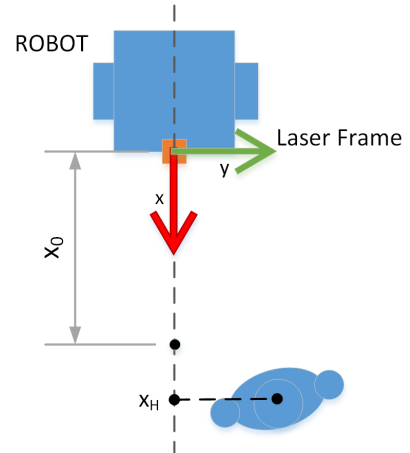


Fig. 4: Depiction of the Laser Frame and the Equilibrium distance  $x_0$

The robot model used is the widely known Unicycle robot, controlled by the inputs  $v_R, \omega_R$  (linear and angular velocities respectively). Rigidly attached to the robot is the *laser frame*, in which the user centroid  $x_H, y_H$  is calculated. The robot's linear velocity is given by,

$$v_R = \lambda(y_H)v(x_H) \quad (2)$$

where,

$$v = \begin{cases} 0 & , x_H > x_0 \\ k_1(x_H - x_0) & , x_2 \leq x_H \leq x_0 \\ v_{walk} & , x_1 \leq x_H \leq x_2 \\ v_{max} - k_2 x_H & , 0 \leq x_H \leq x_1 \end{cases} \quad (3)$$

$$k_1 = \frac{v_{walk}}{x_2 - x_0}, k_2 = \frac{v_{max} - v_{walk}}{x_1}$$

The term  $\lambda$  is a velocity modulating term (see below for a more thorough analysis). Equation (3) defines a piecewise linear velocity profile, consisting of three regions; the *approach region*, the *walking region* and the *collision region*.

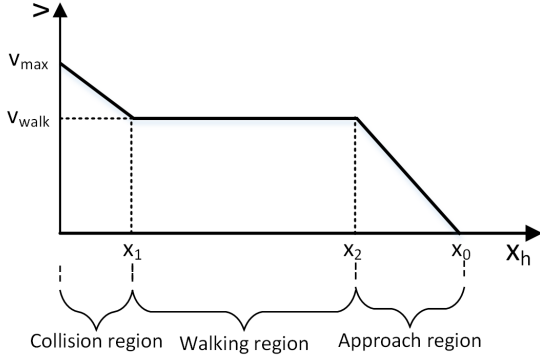


Fig. 5: Profile of the linear velocity input

The *walking region* is the set on the  $x$ -axis of the LRF frame, within which the robot has a constant velocity, namely the walking velocity  $v_{walk}$ . In this region the robot moves synchronously with the user. If the human moves very close to the robot, he/she enters into the *collision region*, in which the robot accelerates up to a maximum velocity  $v_{max}$ . Conversely, if the human falls behind (or enters the HIZ from a distance greater than the Equilibrium distance  $x_0$ ), the *approach region* is considered, where the robot accelerates from halt up to the walking velocity. The second robot input, the angular velocity  $\omega_R$ , is described by the following equations,

$$\omega_R = \begin{cases} 0 & , |y_H| < \varepsilon \\ k_\omega \text{sgn}(y_H)(|y_H| - \varepsilon) & , |y_H| > \varepsilon \end{cases} \quad (4)$$

$$k_\omega = \frac{\omega_{max}}{HIZ_w/2 - \varepsilon}$$

Here  $\omega_{max}$  the maximum angular velocity,  $HIZ_w$  is the width of the HIZ and  $\varepsilon$  is a deadband about the  $x$ -axis. The deadband is inserted in order to filter out natural gait oscillations during walking, as well as noise from the centroid estimator. In our experiments  $\varepsilon$  was set to 10cm.

Using Eq. (4), the robot essentially turns in such a way as to always face the user. During experiments it was observed that in corners the users place themselves on the outer limits of the  $y$ -axis to make the robot turn fast enough. This oversteers the robot and in order to correct its heading, they must swiftly move on the other end of the axis. At

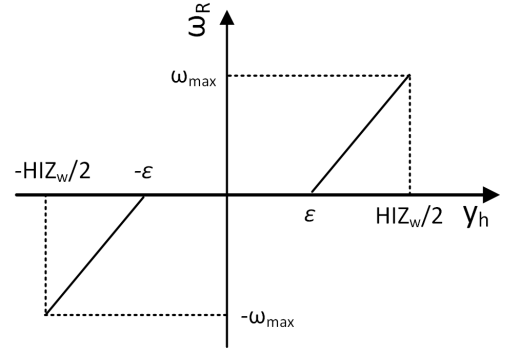


Fig. 6: Profile of the angular velocity input

the same time the robot is moving forward with a linear velocity, making the reaction time rather short and leading to unstable behaviors. To prevent this situation, we have inserted a velocity modulating term  $\lambda(y_h)$  in Eq.(1). The term is given by,

$$\lambda = \begin{cases} 1 & , |y_H| < y_a \\ \frac{y_b - |y_H|}{y_b - y_a} & , y_a \leq |y_H| \leq y_b \\ 0 & , y_b < |y_H| \end{cases} \quad (5)$$

$$y_b = \varepsilon + b(HIZ_w/2 - \varepsilon)$$

$$y_a = \varepsilon + a(HIZ_w/2 - \varepsilon)$$

The parameters  $0 < a < b < 1$  are percentages with respect to the deadband. A graphical depiction of  $\lambda$  can be seen in below.

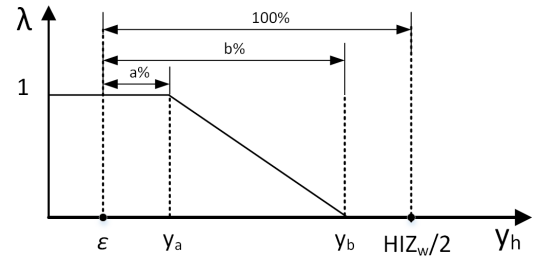


Fig. 7: Illustration of the  $\lambda$  function

The  $\lambda$  term reduces the linear velocity as the user increases his/hers lateral displacement. On the outer regions, the robot halts and turns on the spot to face the human. For our experiments the parameters were set to  $a=0.3$  and  $b=0.6$ .

## IV. EXPERIMENTAL RESULTS

### A. Assessment of HMM-based gait characterisation

1) *Experimental setup and data description:* The experimental results presented in this section are based on data collected during a full-scale experimental study conducted at the premises of Agaplesion Bethanien Hospital - Geriatric Center (University of Heidelberg) at the frames of the EU-funded FP7 research project MOBOT. Patients with moderate to mild impairment, according to pre-specified clinical inclusion criteria, took part in this experiment. The



Fig. 8: Snapshots of a subject walking assisted by the robotic platform, during one stride.

Subject	Stride Time [sec]	Swing Time [sec]	Stride Length [cm]
1	$1.02 \pm 0.04$	$0.38 \pm 0.03$	$74.6 \pm 4.6$
2	$1.04 \pm 0.02$	$0.39 \pm 0.04$	$88.7 \pm 2.9$
3	$1.06 \pm 0.02$	$0.41 \pm 0.04$	$73.7 \pm 1.6$
4	$1.17 \pm 0.06$	$0.45 \pm 0.01$	$72.0 \pm 1.1$
5	$1.17 \pm 0.03$	$0.41 \pm 0.03$	$59.6 \pm 2.3$

TABLE I: Gait parameters (means and standard deviations) computed by the proposed HMM-based methodology for five subjects.

patients were wearing their normal clothes (no need of specific clothing). We have used a Hokuyo Rapid URG laser sensor (UBG-04LX-F01 with mean sampling period of about 28msec), mounted on the robotic platform of Fig. 1 for the detection of the patients' legs (scanning was performed at a horizontal plane below knee level). A GAITRite system was also used to collect ground truth data, which will be used in future work for a formal clinical validation study. GAITRite provides measurements of the spatial and temporal gait parameters and is commonly used for medical diagnosis [15].

The study presented in this paper uses the data from five patients with moderate mobility impairment (aged over 65 years old). Each subject walked straight with physical support of the robotic rollator over a walkway. The HMM was trained by using the recorded data from twelve different patients. All patients performed the experimental scenarios under appropriate carer's supervision. The subjects were instructed to walk as normally as possible. This results in a different walking speed for each subject, and in different gait parameters.

Fig. 8 shows a sequence of snapshots of a subject performing the experimental scenario, captured by a Kinect camera that was also mounted on the robotic rollator (Fig. 1).

2) *HMM Results:* As discussed, the goal of the work presented in this paper is to perform an initial performance assessment of the HMM-based methodology regarding the extraction of gait parameters. We have first isolated the laser data corresponding to the strides performed by each subject on the walkway. These data were then processed to extract the gait parameters using the HMM methodology described in Section II.

Table I contains the statistics of the gait parameters computed as the outcome of the HMM-based gait segmentation and characterisation.

For better demonstrating and assessing the experimental

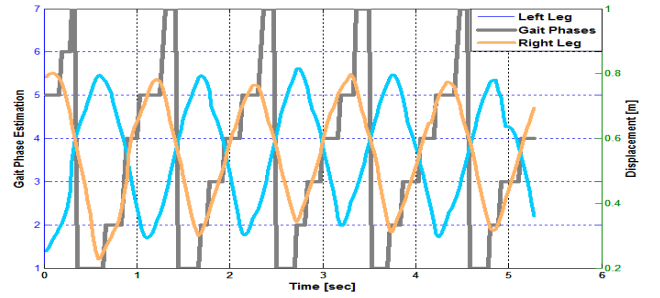


Fig. 9: Experimental Results: Example of an exact gait phase recognition sequence for Subject #2, as estimated by the HMM-based approach. The grey line (axis on the left) depicts the gait phase transition. The blue and orange lines (axis on the right) show the displacement of the left and right leg, respectively, on the sagittal plane.

results obtained, we present as an example the exact gait phase recognition sequence provided by the HMM-based approach for the full duration of the strides performed by one subject (Subject #2). These results are depicted in Fig. 9, where the blue and orange lines show the displacement of the left and right leg in the sagittal plane, respectively, during the five strides (axis on the right), while the grey line depicts the gait phase segmentation extracted by the HMM (axis on the left).

By analysing these results it can be concluded that the gait characterisation performed by the proposed HMM-based methodology manages to provide a reliable outcome in terms of clinically-relevant gait parameters, as can be deduced by the consistency in the extracted gait parameters between consecutive strides within each subject (also related to the standard deviation results). An initial evaluation with ground-truth data demonstrates that the HMM approach provides reliable and valid gait characterisation results, that could be eventually used for further classification of gait properties. Initial comparison with other approaches (e.g. a rule-based methodology based on raw data spatiotemporal filtering) also demonstrates that the added complexity of the HMM approach, w.r.t more basic tracking methodologies, is necessary for improved accuracy. These results are very promising clearly depicting the capacities of the proposed HMM-based methodology to successfully segment the gait cycle and recognize the specific gait phases, extracting comprehensive information about the specific action of each leg, which can be very useful for medical diagnosis. Nevertheless, the results demonstrate that there is significant space for increasing the accuracy of the system. Further comparative analysis and full-scale validation of this methodological framework constitutes one of the main objectives of current research work.

### B. User Following

The user front-following control scheme presented in the previous section, has been implemented on a Pioneer 3DX differential drive robot, with a Hokuyo UBG-04LX-F01 laser

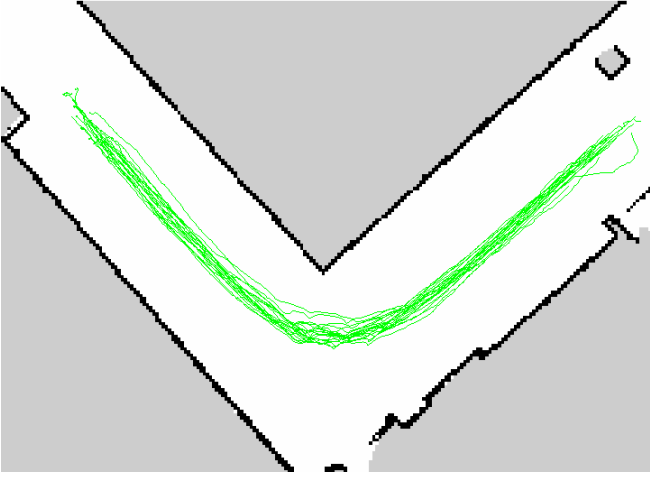


Fig. 10: Traces of the baseline experiments (green). The subjects started on the right and progressed to the left.

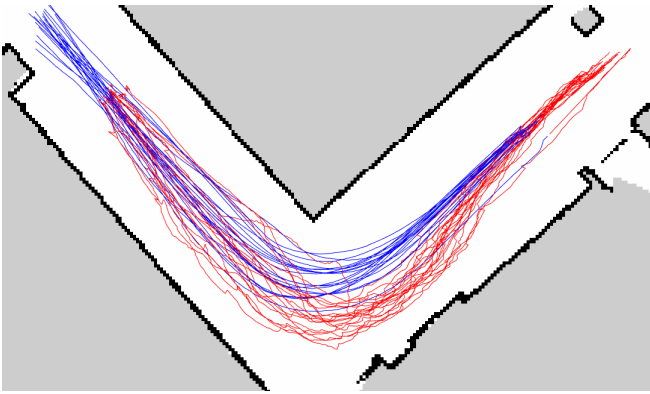


Fig. 11: Traces of the following experiments (Human-red, Robot-blue). The subjects started on the right and progressed to the left

range finder. The experiments considered here, aim to assess the gait pattern of the users with and without the robot following them from the front. Ten healthy subjects were asked to walk naturally from an initial predefined position, around a corner and stop at a designated target position. Each subject performed two runs, thus in total 20 paths were collected as a baseline. The subjects were tracked with the laser scanner on top of the robot, which in turn was placed statically at the head of the corner, overseeing the experimental field. In post processing, using the detection algorithm, the centroid traces were extracted, as seen in Figure 10.

Following, the subjects were asked to perform the experiment again, but with the robot following them from the front. Each subject did two test runs in order to get acquainted with the robot behavior. Then, they performed the experiment twice. The total collected paths are again 20.

To analyze the paths, we have divided the plane into a grid of  $48 \times 26$  square cells with an edge of 20 cm each. Then, for each path we collected the binary mask consisting of those cells that the path has traversed. By counting the

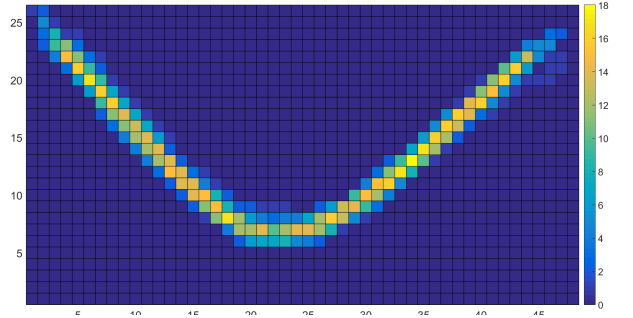


Fig. 12: Histogram of the baseline paths

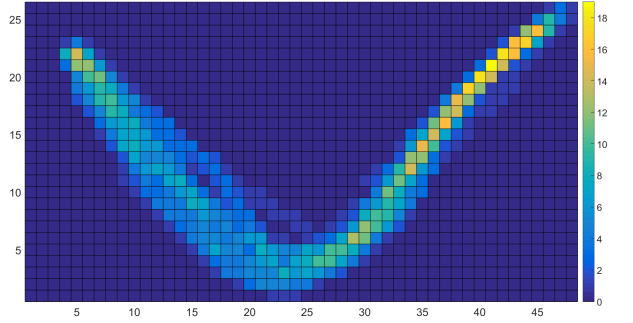


Fig. 13: Histogram of the users' paths (following)

number of masks each cell appears in, we have produced a 2D histogram of those masks. Apparently, since we have 20 paths in each case, the count of each cell goes from zero up to twenty. The three histograms are,

$$\begin{aligned} H_B(i, j) &: \text{Baseline paths} \\ H_U(i, j) &: \text{User paths} \\ H_R(i, j) &: \text{Robot paths} \\ i &\in [1, 48], j \in [1, 26] \end{aligned} \quad (6)$$

The histograms are presented in figures 12-14.

From the three histograms we can produce two new sets of distributions. By dividing the count of each cell with the total number of paths, we produce the probability of each cell being traversed by a path, viz.

$$\begin{aligned} T_B(i, j) &= H_B(i, j)/20 \\ T_U(i, j) &= H_U(i, j)/20 \\ T_R(i, j) &= H_R(i, j)/20 \end{aligned} \quad (7)$$

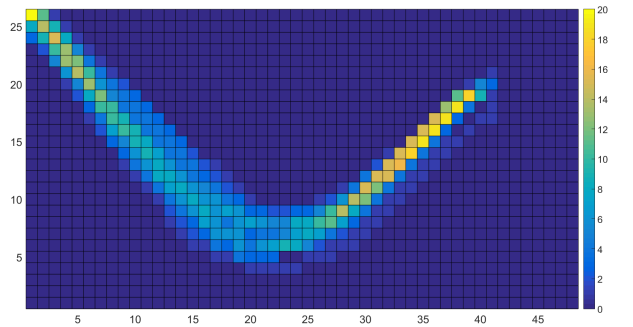


Fig. 14: Histogram of the robot paths (following)

TABLE II: Measure of the extent of the "User" and "Robot" groups with respect to the "Baseline" group

	Count()	% rel. diff.
$T_B$	186	-
$T_U$	318	70.96%
$T_R$	253	36.02%

Thus a cell with high such a probability means that it is traversed by most of the paths. Note that these are not probability distributions as they don't sum up to one. Another set of distributions can be produced by dividing each cell with the total count of its respective histogram, i.e.

$$\begin{aligned} P_B(i, j) &= H_B(i, j) / \sum_{i,j} H_B(i, j) \\ P_U(i, j) &= H_U(i, j) / \sum_{i,j} H_U(i, j) \\ P_R(i, j) &= H_R(i, j) / \sum_{i,j} H_R(i, j) \end{aligned} \quad (8)$$

These express the probability of a user/robot being on a specific cell and are probability density functions. Equations (6),(7),(8) are similar up to a scaling factor (for each group "B", "U", "R"), thus all three have the same shape. To compare the three groups, we resort to the Hellinger distance which is a measure of statistical distance between two distributions P, Q given by,

$$H(p, q) = \frac{1}{\sqrt{2}} \sum_k (\sqrt{p_k} - \sqrt{q_k})^2$$

The Hellinger distance ranges from zero to one, with zero being identical distributions and one completely disjoint. The distances of  $P_U$  to  $P_B$  and  $P_R$  to  $P_B$  are,

$$H(P_U, P_B) = 0.6265, H(P_R, P_B) = 0.4907$$

We see that the Robot path distribution is more similar to the Baseline distribution than the User' distribution. This means that the users actually tend to "drive" the robot to the path they consider "optimal" i.e. the one that *they* would take under normal conditions (the baseline paths). Doing so, they deviate from their normal gait patterns. A measure of dispersion of the histograms is the relative differences between  $count(T_R) - count(T_B)$  and  $count(T_U) - count(T_B)$ , since the count function measures the number of cells a distribution contains. Thus the relative difference is a measure of the extent of a group with respect to the baseline group.

From Table II we see that the users cover almost 71% more cells trying to steer the robot, than when walking normally, which is almost twice the cells the robot covers. This can be regarded as a measure of cognitive load since it shows that the users walk through a wider area.

1) *Current research direction:* Our current research efforts focus on extending the following behavior in unstructured environments. The control has been split into three tasks; *undecidability detection*, *intent identification* and *local planning*. As mentioned earlier, the robot can encounter areas in which there are more that one "distinct" directions e.g. in a T-junction. The robot must be able to discern these

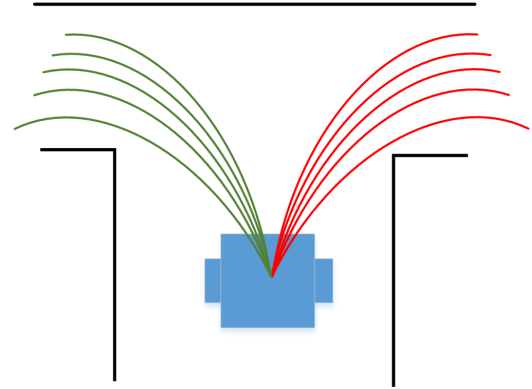


Fig. 15: Equivalence classes for path sets in a T-junction. Red is the "Right" class and Green is the "Left" class

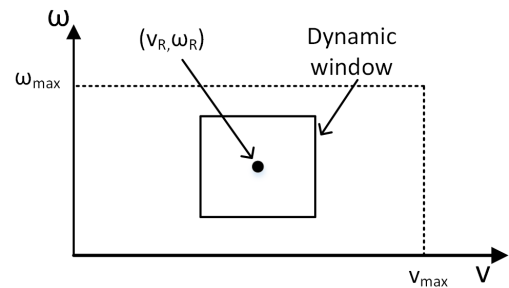


Fig. 16: Dynamic window of constrained input

cases and go into *intent identification* mode, in order to resolve the conundrum it is faced with. Knepper et al. [16], have presented an algorithm based on an extended notion of path-homotopy, in order to produce "equivalence classes" of feasible paths. Formally, two paths are homotopic if there is a continuous deformation which sends one to the other. Strictly speaking, the paths must have the same start and end points. By relaxing the definition, one can speak of "equivalent" paths, that is, paths that have the same starting point and can be continuously deformed to one another. In [16], the algorithm produces feasible paths of a certain length i.e. ones that satisfy the differential equations of the robot, with varying curvature  $\kappa(s)$ . The paths are checked for collision against a costmap and are grouped into classes based on their Hausdorff distance.

Our current approach is similar to [16], albeit simpler. Firstly, we introduce the notion of *dynamic undecidability*. This is based on the fact that, as the robot moves, the feasible paths are constrained by the kinodynamic bounds of the system. For example, if the robot is moving fast, a sharp turn might be unfeasible. Thus, in a T-Junction, it might be the case that only one direction is actually feasible. Following the widely used *Dynamic Window Approach* in local planning, we produce paths of *constant* curvature, sampling from a dynamic window of the input space  $(v, \omega)$ .

The curvatures are checked for collision against a moving costmap centered around the robot, which is created by laser range scans. Following the free paths are clustered together

based on their curvature separation (simple 1D clustering).

Given the available clusters, if there is more than one available direction, the robot enters into the *intent identification* mode, slowing down and observing the human. It uses the kinematic controller and produces a set of control inputs ( $v_H, \omega_H$ ), resulting to a curvature  $\kappa_H$ . When the human gets close to robot, under a predefined distance, the controller selects the closest cluster to  $\kappa_H$ , and feeds the median free path to a local planner, as a “global path”. This ensures a collision-free trajectory of the robot, which moves towards the human direction.

## V. CONCLUSION AND FUTURE WORK

This paper presents current research work that aims at the development of an intelligent robotic rollator to provide user-adaptive and context-aware walking assistance. To achieve such targets, a large spectrum of multimodal sensory processing and interactive control modules need to be developed and seamlessly integrated. This paper focuses on user-oriented human-robot interaction and control, by which we refer to the functionalities that couple the motions, the actions and, in more general terms, the behaviours of the assistive robotic device to the user in a *non-physical interaction* context. The paper summarizes recent research advances and scientific challenges aiming towards two complementary directions: 1) the first one addresses the development of a reliable gait tracking and classification system, for which we propose an approach based on HMMs, which can operate online by processing raw sensorial data provided by an onboard laser rangefinder sensor, and 2) the second one regards the development of a control system that can support a ‘user-following’ behaviour, that is, enable the robotic rollator to follow and comply to the walking characteristics of the user without any physical interaction (i.e. without any force being applied on the handles of the Rollator) and remain in close vicinity to the user in case of need.

This paper summarizes the theoretical framework and presents current experimental results obtained using real data both from patients (elderly subjects with mild to moderate walking impairments) and normal subjects. In particular, we perform an initial assessment of the gait characterisation performance achieved by the proposed HMM-based methodology, and demonstrate that this approach manages to provide a reliable outcome in terms of extracting clinically-relevant gait parameters. These results are very promising clearly depicting the capacities of the proposed HMM-based methodology to successfully segment the gait cycle and recognize the specific gait phases, extracting comprehensive information about the specific action of each leg, which can be very useful for medical diagnosis. Nevertheless, the results demonstrate that there is significant space for increasing the accuracy of the system. Further comparative analysis and full-scale validation of this methodological framework constitutes one of the main objectives of current research work. Furthermore, we demonstrate the applicability of a user front-following interactive control behaviour based on a virtual force field that enables the robotic rollator to provide

adaptive assistance to the walking user. The main scientific challenge here is to detect the user intention and develop a shared control framework that can provide intuitive mobility assistance while reducing the cognitive load of the user.

Combining work in all these research directions, our ultimate goal is to develop assistive robotic technologies that can both monitor user actions (in order for instance to detect in real time specific gait pathologies and automatically classify the patient status or the rehabilitation progress) and provide effective, user-adaptive and context-aware, active mobility support.

## REFERENCES

- [1] USCensus, “The elderly population,” 2010.
- [2] T. Herman, N. Giladi, T. Gurevich, and J. Hausdorff, “Gait instability and fractal dynamics of older adults with a cautious gait: why do certain older adults walk fearfully?” *Gait Posture*, vol. 21, no. 2, pp. 178 – 185, 2005. [Online]. Available: <http://www.sciencedirect.com/science/article/pii/S0966636204000438>
- [3] P. D. Foundation, “Statistics for parkinson’s disease,” 2010. [Online]. Available: <http://www.pdf.org>
- [4] S. Center, “Stroke statistics,” 2010. [Online]. Available: <http://www.strokecenter.org>
- [5] P. Brezillon, “Context in problem solving: A survey,” *The Knowledge Engineering Review*, vol. 14, pp. 1–34, 1999.
- [6] X. Papageorgiou, G. Chalvatzaki, C. Tzafestas, and P. Maragos, “Hidden markov modeling of human normal gait using laser range finder for a mobility assistance robot,” in *Proc. of the 2014 IEEE Int’l Conf. on Robotics and Automation*.
- [7] —, “Hidden markov modeling of human pathological gait using laser range finder for an assisted living intelligent robotic walker,” in *Proc. of the 2015 IEEE Int’l Conf. on Intelligent Robots and Systems*.
- [8] R. W. Kressig, R. J. Gregor, A. Oliver, D. Waddell, W. Smith, M. OGrady, A. T. Curns, M. Kutner, and S. L. Wolf, “Temporal and spatial features of gait in older adults transitioning to frailty,” *Gait Posture*, vol. 20, no. 1, pp. 30 – 35, 2004. [Online]. Available: <http://www.sciencedirect.com/science/article/pii/S0966636203000894>
- [9] A. Muro-de-la Herran, B. Garcia-Zapirain, and A. Mendez-Zorrilla, “Gait analysis methods: An overview of wearable and non-wearable systems, highlighting clinical applications,” *Sensors*, vol. 14, no. 2, p. 3362, 2014. [Online]. Available: <http://www.mdpi.com/1424-8220/14/2/3362>
- [10] E.-J. Jung, B.-J. Yi, and S. Yuta, “Control algorithms for a mobile robot tracking a human in front,” in *Intelligent Robots and Systems (IROS), 2012 IEEE/RSJ International Conference on*, Oct 2012, pp. 2411–2416.
- [11] D. Ho, J.-S. Hu, and J.-J. Wang, “Behavior control of the mobile robot for accompanying in front of a human,” in *Advanced Intelligent Mechatronics (AIM), 2012 IEEE/ASME International Conference on*, July 2012, pp. 377–382.
- [12] G. Arechavaleta, J.-P. Laumond, H. Hicheur, and A. Berthoz, “The nonholonomic nature of human locomotion: a modeling study,” in *Biomedical Robotics and Biomechanics, 2006. BioRob 2006. The First IEEE/RAS-EMBS International Conference on*, Feb 2006, pp. 158–163.
- [13] —, “On the nonholonomic nature of human locomotion,” *Autonomous Robots*, vol. 25, no. 1-2, pp. 25–35, 2008. [Online]. Available: <http://dx.doi.org/10.1007/s10514-007-9075-2>
- [14] C. A. Cifuentes, A. Frizzera, R. Carelli, and T. Bastos, “Human?robot interaction based on wearable {IMU} sensor and laser range finder,” *Robotics and Autonomous Systems*, vol. 62, no. 10, pp. 1425 – 1439, 2014.
- [15] A. Rampp, J. Barth, S. Schuelein, K.-G. Gassmann, J. Klucken, and B. Eskofier, “Inertial sensor-based stride parameter calculation from gait sequences in geriatric patients,” *Biomedical Engineering, IEEE Transactions on*, vol. 62, no. 4, pp. 1089–1097, April 2015.
- [16] R. Knepper, S. Srinivasa, and M. Mason, “An equivalence relation for local path sets,” in *Algorithmic Foundations of Robotics IX*, ser. Springer Tracts in Advanced Robotics, D. Hsu, V. Isler, J.-C. Latombe, and M. Lin, Eds. Springer Berlin Heidelberg, 2011, vol. 68, pp. 19–35. [Online]. Available: [http://dx.doi.org/10.1007/978-3-642-17452-0\\_2](http://dx.doi.org/10.1007/978-3-642-17452-0_2)